High speed imaging and algorithms for non-invasive vibrations measurement

David Mas, Julian Espinosa, Jorge Perez, Carlos Illueca
University of Alicante, Inst. Optics Applied to the Sciences and Technologies, Alicante, Spain

Belen Ferrer
University of Alicante, Dep. Civil Engineering, Alicante, Spain

Ana B, Roig
University of Alicante, Dep. Optics, Alicante, Spain

ABSTRACT: Analysis of vibrations and displacements is a hot topic in structural engineering. Video cameras can provide good accuracy at reasonable cost. Proper system configuration and adequate image processing algorithms provide a reliable method for measuring vibrations and displacements in structures. We propose using a high speed camera for measuring small vibrations in a column after an impact. We show that vibrations with amplitudes smaller than 0.1 mm can be registered with a good accuracy. The method can be applied on standard commercial cameras, thus resulting in a reliable cost-effective method.

1 INTRODUCTION

Monitoring of vibrations and displacements of structures under dynamic excitations or impacts is of major importance in structural engineering Usually, contact instrumentation is used to analyse the dynamics of a vibrating body, but there are occasions where security requirements, accessibility or special characteristics of the structure recommend the use of non-contact devices.

Common non-contact devices like laser vibrometers and high-speed laser interferometers provide a reliable solution for a wide variety of applications (Castellini et al. 2006, Bartoli et al. 2008), but their cost tend to be very high and they are not cost-effective for many applications.

Video cameras can provide good accuracy at reasonable cost. Proper system configuration and adequate image processing algorithms provide a reliable method for measuring vibrations and displacements in structures. Recently, some of the authors of this communication presented a new method for measuring displacements in a column under an impact (Ferrer et al. 2011): a cross target was attached to the structure under study (a column) and then, an impulsive load was applied on it. A high speed camera registered the movement of the target. The complete set of video images was stacked on a hypermatrix, and a temporal re-slice was performed. From the obtained profile, the position of the target was obtained and could be easily calculated. Although it provided good results, we found that the obtained spatial resolution was strongly limited by the camera sensor and thus an alternative proposal is needed.

Determining the accuracy of an imaging system is difficult due to the variety of situations where the method is applicable. Three factors need to be taken into account: camera resolution, distance to the target and camera objective. Adequate combination of these factors will determine the accuracy of the measurements and the limitation of the system, which have to be adjusted according to the expected displacement distances.

Resolution of the camera is linked to the speed. Due to hardware limitations video cameras are, in general, unable to provide high temporal and spatial resolutions simultaneously. Although still-cameras can provide resolutions above 12 Mpx, commercial video cameras rarely provide resolutions larger than 2 Mpx with acquiring speeds below 60 frames per second (fps).

Higher acquisition rates are commonly achieved at the expense of the spatial resolution. In the case above described we used an AOS X-PRI camera working at 1000 fps with a resolution of 800×600, i.e. less than 0.5 Mpx. Although cameras working at these rates with better spatial resolutions can be found, their price tends to be very high thus not being cost-effective for many engineering applications.

Distance between the camera and the target is imposed by the specific structure to be measured. Accessibility, security or even needs of mechanical isolation may determine the working distance and thus may be considered as a boundary condition, with limited improvement possibilities.

The objective lens of the camera can overcome some of the limitations above exposed. In order to obtain good imaging, the optics has to be luminous and provide good magnification. With proper magnification, the target can be brought closer and thus the ratio of pixels per mm can be increased. In opposition to the limited stock of high speed cameras, the choice and configurations of objectives is very wide. The camera can be coupled either to microscopes and telescopes and thus the method can be applied to different problems.

As we said above, proper combination of the three factors allow to construct an optimal system. From all of them, the real bottleneck of the process is the sensor resolution. Our aim in this communication is to implement a method that increases the accuracy of the sensor by post-processing the video sequence. The method is based on a convenient design of the target to be tracked. The object to be detected consists on a simple ellipse over a uniform background. Restrictions on the target shape leads to a method which allows obtaining the geometrical centre of the ellipse with subpixel resolution, i.e. with accuracy above than that provided by the camera sensor.

In what follows, we will present the subpixel method for object tracking and we will discuss about its possibilities. The method will be first checked on lab experiments. Then, we will apply the technique on a real simple structure. Results will be confirmed by a Finite Element Model (FEM) of the structure and by independent measurements. Finally, we will outline the main conclusions and discuss about future developments of the method.

2 METHODS

2.1 Simple object tracking

Subpixel techniques increase the nominal resolution of the image sensors by digitally post-processing the captured images. Basically, these techniques consist of smart interpolation of image features. In (Shortis et al.1994) and (Shortis et al. 1995) the authors present different methods for target recognition and location. From both tasks, target recognition is the most complicated one since a proper analysis and segmentation of the image is necessary. This process is simplified and accelerated by using specific targets that are easy to recognize (Bruckstein and O'Gorman, 1998). Typically, circles or ellipses are used.

The method used here is simple and it briefly consists of attaching to the moving object a target with an elliptical shape and registering a video sequence. Tracking is performed by fitting the extracted contours from each frame of the sequence to the general ellipse equation

$$Ax^2 + Bxy + Cy^2 + Dx + Ey + F = 0 \tag{1}$$

From the fitting, we obtain the centre of the ellipse:

$$(x_c, y_c) = \left(\frac{-D}{2A}, \frac{-E}{2C}\right) \tag{2}$$

In order to check the real performance of our proposal, a lab experiment has been performed. An elliptical target is attached to a rotating plate. The plate rotates at an angular speed of 200 deg/s. (see figure 1a). The camera was placed at 2 m from the target, being the imaged ellipse size of 45×106 pixels with a resolution of 0.903 px/mm.

Frame processing starts by manually selecting a point inside the ellipse in the first frame. From the gray values in the local region around this point, a threshold is calculated and the whole image is binarized. The dark line around this seed-point is detected and extracted through

mathematical morphology boundary tracing (Serra, 1983). Dots belonging to the line are then fitted to equation (1), thus obtaining the ellipse parameters and centre (eq. 2). The centre of each ellipse is used as the seed point for the following frame, so the process becomes automatic.

(a)

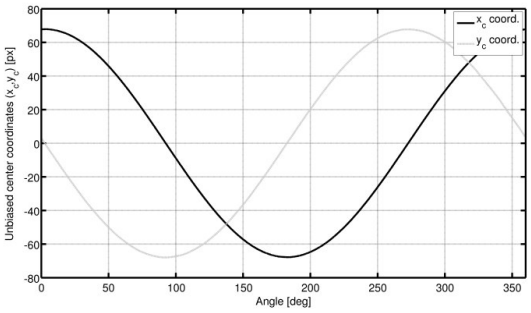

(b)

Figure 1: (a) Target used for subpixel ellipse tracking (b) Unbiased coordinates of the ellipse centre.

In figure 1b we represent the coordinates of the ellipse centre throughout the full sequence. In order to facilitate representation and direct comparison, we depict the difference from their mean value. According to the circular movement, the unbiased centre coordinates (x_c, y_c) follow a trajectory in the form $(A\cos(\omega\alpha+\phi), A\sin(\omega\alpha+\phi))$, where A corresponds to the rotation radius and α is the angle where the ellipse should be located, which can be easily determined from the rotating speed and the time. If the ellipse is correctly located, ω and ϕ should theoretically be equal the one and zero, respectively. Least square fitting of the trajectory for both coordinates provide the following values, where the 95% confidence bounds are given between in brackets:

$$
\begin{aligned}
x_c \rightarrow \quad & A = 67.84 \text{ px} && [67.83, 67.84] \\
& \omega = 0.99924 \text{ deg}^{-1} && [0.99924, 0.99925] \\
& \phi = -2.48435 \text{ deg} && [-2.49179, -2.47690] \\
y_c \rightarrow \quad & A = 67.80 \text{ px} && [67.80, 67.81] \\
& \omega = 0.99867 \text{ deg}^{-1} && [0.99867, 0.99934] \\
& \phi = -2.58977 \text{ deg} && [-2.58978, -2.58977]
\end{aligned}
\tag{3}
$$

The correlation coefficient for both fittings has been equal to one, while the residuals between the measured and the expected values have been -0.010 ± 0.059 px, for x_c , and -0.002 ± 0.059 px for y_c (mean ± standard deviation). The correspondence between results for both coordinates shows the consistency of the method. The values obtained for ϕ only show a zero error that can be corrected by a re-calibration of the system. The values obtained for ω and the narrowness of the confidence intervals also show the reliability of the method.

The small residuals obtained between the real and expected position show that the method is able to localize the target with high subpixel accuracy. By considering that the target is correctly detected while it is located in a band of three times the standard deviation around the expected value ($\pm 3 \times STD$), we obtain that the accuracy of the method can be set in 0.18 px. Taking into account the px/mm ratio the method is able to track movements of 0.2 mm from 2 m, or equivalently an angular resolution of 20 arcsec.

2.2 Far object tracking

As we said in the introduction, by a convenient selection of the objective lens, the final resolution can be very much increased. In a second experiment, a circular object has been situated 13 m from the camera in order to impose a low-resolution of 0.65 px/mm, resulting a diameter for the

captured target of 33 px. During the sequence, the target was manually shifted with a micrometric screw 5 mm left and right from the initial position. The sequence is processed off-line as it was explained above. In figure we show in grey colour the displacement when nominal resolution pixel of the circle is considered. One can see that the structure of the movement is quite rough and no additional information apart from the total displacement can be obtained. The results obtained from the centre of the fitted circle are also plotted in black. It is remarkable that the curve is much smoother and even the pauses in the manipulation of the screw are detected.

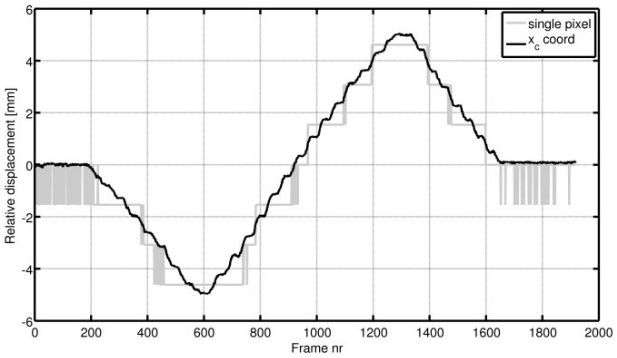

Figure 2: Target movement detection from tracking a moving target with pixel accuracy (gray) or supixel accuracy (black).

Resolution has been determined by evaluating the position error when the target is static. Now, a resolution of 0.08 px is achieved, which means that 0.13 mm are detected. Considering the distance from the camera to the target, the angular resolution is around 2 arcsec. This resolution can be improved by post processing the signal, i.e. a simple smoothing filter over the signal here presented increases the resolution to 0.06 px (1.5 arcsec). This experiment shows the possibilities in measuring displacements at medium distance range, and thus its application in real experiments in structural mechanics.

3 EXPERIMENTAL RESULTS

3.1 Vibrations on a small structure

The subpixel method has now been applied to the measurement of the main vibration parameters of a column in a small structure. We selected a steel column of 2.1 m high composed by two welded UPN-100 beams forming a hollow column. The two ends of the column are pinned to the floor and to one larger structure (emergency stairs) A steel ball of 0.44 kg was used as projectile for the impact. The ball was mounted in a pendulum of 1.5 m hanging from the upper part of the column. By releasing the ball from a distance of 90 cm from the column, we achieved an impact at 2.3 m/s. The vibration produced by the impact was registered by the high speed camera focusing on a target attached to the column.

(a) (b)

Figure 3: (a) Steel column under analysis (b) Camera and target used for vibration monitoring.

Prior to the experimental analysis the problem was implemented in a Finite Element Model (FEM) and a modal and dynamic analysis was performed. The FEM was created in LSDYNA code. The column was modelled with SOLID element. The steel was modelled as an elastic-plastic material with a Young modulus of 210 GPa, Poisson modulus 0.3, density 7850 kg/m^3 and yield strength 275 MPa. The column was modelled as a two pinned beam. A modal analysis was performed to find the main vibration modes. The frequencies (in Hertz) of the first six modes are shown in table 1.

Table 1 Vibration modes for the steel column in the finite element model.

Mode	Frequency (Hz)	Movement description
1	66.87	Displacement, y direction,1/2 wavelenght
2	71.21	Displacement, x direction, 1/2 wavelenght
3	261.31	Displacement, y direction, 1 wavelenght
4	274.92	Displacement, x direction, 1 wavelenght
5	566.36	Displacement, y direction, 3/2 wavelenght
6	584.84	Displacement, x direction, 3/2 wavelenght

In order to perform the dynamic analysis, a spherical ball was modelled hanging by a wire of 1 mm of diameter fixed to the upper part of the column. Figure 4 shows the complete model for dynamic calculations. In both modal and dynamic analyses, the y axis match the direction of the impact and the z axis is vertical.

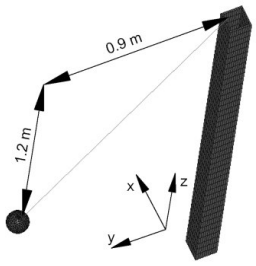

Figure 4: Schematic representation of the experiment for the dynamic simulation.

Through the numerical dynamic analysis, we found the displacement of the all nodes and, in particular, of the one situated at the same height of the point of impact and in the exterior x surface of the column. This displacement is shown in figure 5. Fourier analysis of the signal provides information about the main modes being excited with the impact. In this case the vibration resulted to be monomodal and corresponds to the first mode of the vibration analysis (see Table 1). Thus, the movement can be easily described as an attenuated oscillation:

$$x(t) = Ae^{-\mu t}\sin(2\pi ft + \phi) \tag{4}$$

where A is the amplitude of the oscillation, f is the linear frequency, μ is the attenuation constant, and ϕ is a boundary constant. Data form the dynamic simulation has been fitted to eq. (4) thus obtaining the values in expression (5) for the parameters (with 95% confidence bounds), in which the subindex d refers to the dynamic simulation, with a correlation coefficient $r^2 = 0.9917$. The confidence bounds are shown between brackets.

$$\begin{aligned} A_d &= 0.0933 \text{ mm} \quad [0.0936,\ 0.0943] \\ \phi_d &= 1.572 \text{ rad} \quad [1.568,\ 1.575] \\ \mu_d &= 14.61 \text{ s}^{-1} \quad [14.60,\ 14.75] \\ f_d &= 66.7 \text{ Hz} \quad [66.5,\ 66.8] \end{aligned} \tag{5}$$

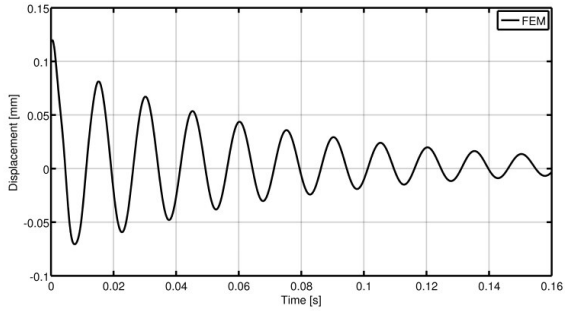

Figure 5: Displacement of a column node situated on the opposite surface of the impact point.

The movement of the column after a real impulsive load was analysed by tracking the target. Experimental implementation consisted in detecting and isolating the circular external bounds of the target in figure 3b. Each pixel belonging to the contour line can be considered as a data point and the whole set can be fitted to the expression in eq.(1). Doing so, the centre of the figure was obtained and movement of the column was measured from the horizontal coordinate. As in the previous case, Fourier analysis of the movement showed that real vibration of the column was monomodal. Therefore results obtained from the coordinate x_c were fitted to the equation (4). In figure 6, we depict an example of the obtained data together with the fitting graph (a monomodal attenuated oscillation).

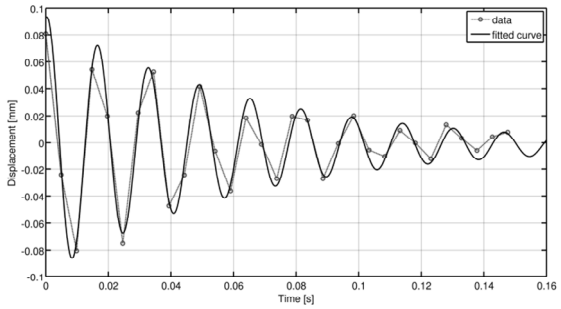

Figure 6: Target displacement measured by target tracking.

In Table 2, we show the values obtained for three tests performed together with the 95% confidence bounds. The value for the constant ϕ has been omitted from the analysis since it is different for each case and does not add any relevant information.

Table 2: Experimental values obtained for the column vibration in eq. (4)

	A(mm)	μ (s^{-1})	f (Hz)	r^2
Test 1	0.102 [0.090, 0.114]	15.7 [12.8, 18.6]	61.8 [61.3, 62.3]	0.9584
Test 2	0.103 [0.089, 0.117]	15.6 [12.5, 18.7]	61.0 [60.5, 61.5]	0.9548
Test 3	0.103 [0.093, 0.114]	15.8 [13.2, 18.3]	61.3 [60.9, 61.6]	0.9693

One can see in the table that there is a full coincidence between results obtained by the camera and those simulated through LSDYNA in expression (5). Displacement of the frequency may be due to small differences in boundary conditions between the model and the real structure.

In order to have an additional experimental confirmation of our results, the data obtained with the high speed camera have been compared with those provided by an accelerometer attached to the column. The existence in the structure of the mode at 64 Hz was checked through a structural accelerometer (333B50 PCB Piezotronics), with a measurement range of ±5g and a frequency range from 0.5 to 3000 Hz. Additionally, the vibration modes were measured by a different image-based technique and similar results were obtained (Ferrer et al. 2011).

3.2 Applications in impact tests

The method here presented was used in a real scale experiment for testing building structures under low speed car impacts (Ferrer et al. 2010). The aim of the experiment was to register the maximum displacement and vibration modes of a concrete column. This parameter is important for analyzing the stresses on the structure under dynamic loading. In figure 7, we show a picture of the crash test together with the displacement registered by the camera. The column was monitorized through several accelerometers, linear displacement sensors and the high speed camera. Accelerometers provided valuable information about vibration modes, but the noise in the signal did not allow double integration for displacement calculation. Linear displacement sensors also failed, since the vibration of the parallel structure to which they were attached was not stable enough. Only data obtained from the camera were reliable and allowed us to obtain the maximum displacement. Moreover, vibration modes obtained from the camera were in coincidence with those obtained with the accelerometers, thus showing the usefulness of the proposed method for direct measuring real displacements.

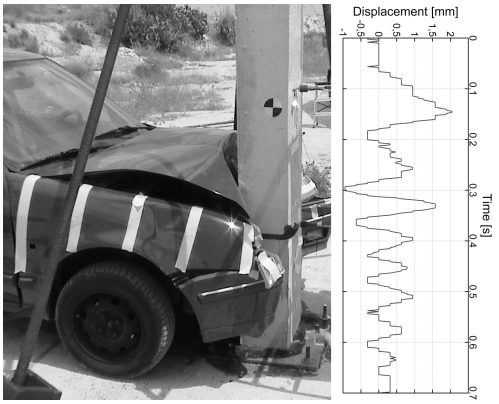

Figure7: Impact test of structural response under low-speed impacts. The graph shows the real displacement registered by the camera.

4 CONCLUSIONS

We have used an image based method for object tracking and vibrations monitoring. By a convenient selection of the target and digitally post-processing acquired video sequences it is possible to obtain to track objects shifts with enhanced resolution, thus allowing fine movement detection. Experiments show that we are able to increase the nominal resolution of the digital sensor in at least one order of magnitude, thus permitting detecting displacements of 0.1 mm from a distance of 13 m. The method has been used to obtain the main vibration parameters of a steel column. Additionally, we introduced its utility for movement monitoring of concrete structure under heavy impulsive loads (car crashing).

This method can be useful in the measurement of displacement of structures as bridges under rail traffic, buildings under earthquake or slender structures subjected to the wind, where contact measurements are difficult or even impossible.

Notice that no previous calibration of the imaging setup has been done, since all detected movements are relative. If one is interested in obtaining absolute values of displacement, the real size of the target should be used in order to obtain the pixel to millimeter conversion. Apart from this conversion, and while the target shape is not optically distorted, no additional considerations are needed.

The distinctiveness fact that the movement of the studied point can be directly seen with a simple procedure helps very much to interpret results. All this features make this method interesting and powerful to the study of the behavior of the structures during dynamic excitation.

Finally we would like to emphasize that although the camera here used is somehow

expensive, the same experiment can be implemented with a camera taking 200 fps, and with lower resolution thus making a low cost, fast and accurate method to analyze the movement of a structure.

ACKNOWLEDGMENTS

The authors would like to acknowledge the financial support of the Spanish Ministerio de Ciencia e Innovacion through the project FIS2009-05639-ET, the Generalitat Valenciana through the project PROMETEO/2011/021 and the University of Alicante through the project GRE10-09. A. B. Roig acknowledges a grant from the Fundacion Cajamurcia.

REFERENCES

Bartoli G., Facchini L., Pieraccini M., Fratini M., Atzeni C. 2008. Experimental utilization of interferometric radar techniques for structural monitoring. Struct. Control Health Monit. **15** p. 283-298.

Castellini P., Martarelli M., Tomasini E.P. 2006. Laser Doppler Vibrometry: Development of advanced solutions answering to technology's needs. *Mech. Syst. Signal Pr.* **20**, p 1265-1285.

Bruckstein A.M., O'Gorman A., 1998. Design of shapes for precise Image registration *IEEE T. Inform. Theory*, **44** p. 3156-3162.

Ferrer B., Ivorra S., Irles R,. Mas D., 2010 Real size experiments of car crash against building column, *WIT Transactions on the Built Environment* **103** p.231-241.

Ferrer B. Espinosa J., Perez J., Ivorra S., Mas D., 2011. Optical scanning for structural vibration measurement *Res. Nondestruct. Eval.* **22**, p 61-75.

Serra J. 1983 *Image Analysis and Mathematical Morphology* Orlando (FL), Academic Press, Inc.

Shortis M.R., Clarke T.A., Short T.A., 1994. A comparison of some techniques for the subpixel location of discrete target image *Proc. SPIE* **2350** p. 230-250.

Shortis M.R., Clarke T.A., Robson S. 1995. Practical testing of the precision and accuracy of target image centring algorithms *Proc. SPIE* **2598**, p. 65-75.